P6.17 SENSITIVITY OF LOWER-TROPOSPHERIC POTENTIAL VORTICITY MAXIMA TO MODEL PHYSICS

C. Michael Trexler and G. M. Lackmann
North Carolina State University, Raleigh, North Carolina

1. INTRODUCTION

That quantitative precipitation forecasting (QPF) is a weakness in modern numerical weather prediction is widely recognized. However, the repercussions of QPF errors for other aspects of operational numerical forecasts remain largely unknown. This problem is especially acute when sub-grid scale precipitation is involved, owing to the fact that the interactions between cumulus parameterization schemes (CPSs) and grid scale processes are complex and have received little in the way of research attention (Wang and Seaman 1997). A useful diagnostic approach for the study of dynamical feedbacks associated with QPF error is the potential vorticity (PV) framework. In this study, we examine the sensitivity of diabatic PV redistribution to the choice of CPS.

Recent observational studies have documented the contribution of diabatic processes to the PV distribution in extratropical cyclones, and have demonstrated that these PV features represent an important element in cyclone evolution (e.g., Davis 1992; Reed et al. 1992; Davis et al. 1993; Stoelinga 1996). These studies identify four primary PV centers in extratropical cyclones: (i) an upper-level PV maximum of stratospheric origin; (ii) a lower boundary warm anomaly (surrogate PV maximum); (iii) a diabatically produced lower-tropospheric PV maximum, which is often most prominent in the warm-frontal region north and northeast east of the cyclone center, and (iv) an upper-tropospheric negative PV center that is also the by-product of diabatic processes. As Raymond (1992) and others have demonstrated, diabatic processes result in a redistribution of PV along the absolute vorticity vector; in strongly sheared midlatitude environments, a considerable offset between the upper negative and lower positive PV extrema is often observed.

Although the lower warm-frontal PV maximum is often of greater amplitude, cyclones that are accompanied by prominent cold-frontal rain bands exhibit an elongated lower-tropospheric PV maximum in the vicinity of cold front. These bands appear to be of critical importance because (i), their location at the western extremity of the warm sector renders them especially effective in northward moisture transport, and (ii) their oft-convective nature makes their representation in numerical forecasts problematic. Earlier studies have indicated that these bands make a substantial contribution to the strength of the low-level jet (LLJ) and warm-sector moisture transport (Lackmann and Gyakum 1999; Lackmann 2001).

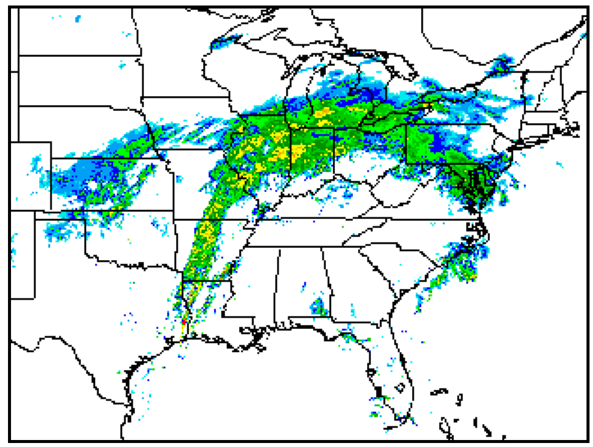

Figure 1: Composite base level reflectivity from NWS Doppler radar, valid 2245 UTC 26 February 1997.

It is hypothesized that model representation of the diabatic cold-frontal PV maximum is sensitive to the choice of convective parameterization scheme (CPS) and perhaps also to details of the grid scale precipitation scheme. Towards the ultimate goal of determining which existing CPS best represents diabatic redistribution of PV in organized convective systems, this study examines the sensitivity of the lower PV maximum to the choice of CPS. The Penn State/NCAR MM5 model was used to conduct a series of sensitivity experiments.

2. CASE OVERVIEW

A case from February 1997 was selected for detailed analysis based on the presence of a strong LLJ, and a prominent cold-frontal rain band (Fig. 1). The strong LLJ was associated with a severe windstorm across parts of Ohio and New York State, and flooding rains were observed north of the system. In this study, we focus on the period of time between 0000 and 0600 UTC 27 February 1997 (hereafter 00/27 and 06/27). At 00/27, a cyclone was centered near the Missouri-Arkansas border, with a trailing cold front extending into the northwestern Gulf of Mexico (Fig. 2). Radar imagery confirms the presence of significant precipitation in the vicinity of the front (Fig. 1). Figure 3 depicts the Eta-analyzed sea level pressure and 950–800 hPa PV; this figure reveals an elongated band of PV in excess of 0.5 PVU extending from near the cyclone center along the cold front. Another cyclonic PV maximum is located west of the cyclone. The 24-h Eta forecast of sea level pressure and lower-tropospheric PV is provided in Fig. 4. The cold-frontal PV band is absent in this forecast, as it was in subsequent operational runs. Errors in operational Eta model forecasts from this case are consistent with a negative bias in the prognosis of the cold-frontal PV maximum. Potential vorticity budget results (not shown) confirm that latent heat release was a prominent factor in the development and propagation of the lower PV maximum, and potential vorticity inversion demonstrates that this feature contributed up to 25% to the strength of the LLJ in that case (Lackmann 2001).

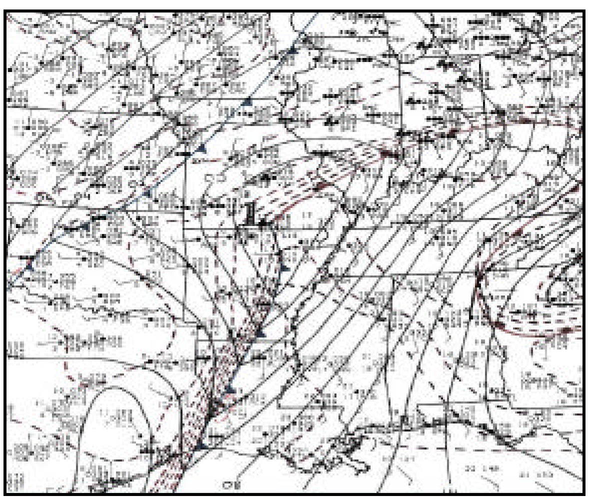

Figure 2. Manually analyzed sea level pressure (solid, 2 hPa contour interval), fronts (usual symbols), and equivalent potential temperature (dashed, contour interval 5K), with surface observations superimposed (standard plotting convention).

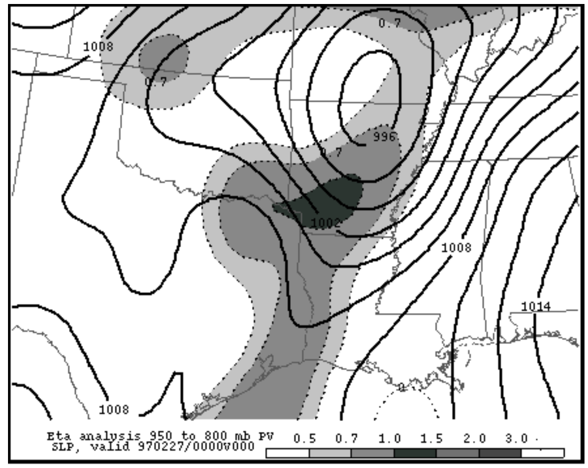

Figure 3: Eta analysis of sea-level pressure (solid, contour interval 2 hPa) and 950-800 hPa potential vorticity (shaded and dashed contours, contour interval 0.2 PVU, shaded as in legend at bottom of panel) valid 0000 UTC 27 February 1997.

The PSU/NCAR MM5 version 3.3 mesoscale model was used to run a series of experiments to test the sensitivity of the lower PV maximum to the choice of CPS for this case. Identical initial and boundary conditions were employed in each experiment. In an effort to maintain relevance to the operational Eta model, the MM5 initial and boundary fields were derived directly from operational Eta model analyses. The experiments included an inner grid with 25-km grid spacing nested within a 75-km grid, as shown in Fig. 5.

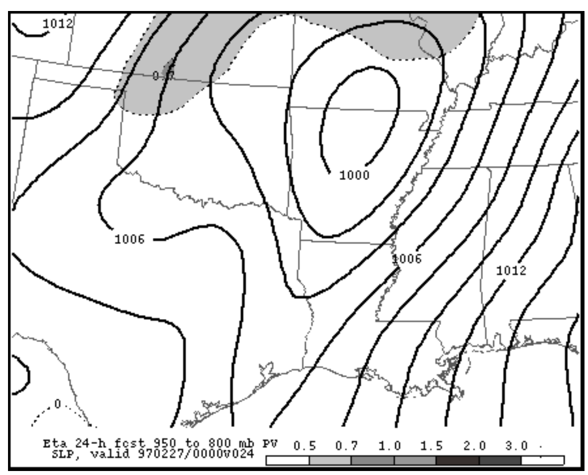

Figure 4. As in Fig. 3, except for 36-hour Eta forecast, valid 0000 UTC 27 February 1997.

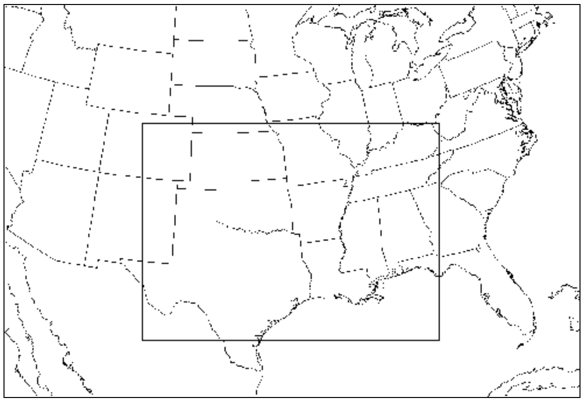

Figure 5: Inner and outer domains used in MM5 sensitivity experiments.

Experiments include a control run using the Betts-Miller CPS, a run in which latent heating was set to zero (fake dry run), and runs utilizing the Grell and Kain-Fritsch CPS.

3. RESULTS

Cold-frontal convection and associated lower-tropospheric PV growth in the MM5 simulations of this case proved to be more highly dependent upon the initial conditions than CPS. The control simulation, which utilized the Betts-Miller CPS, successfully produced a cold-frontal PV maximum which corresponded with that shown in the Eta analysis (cf. Figs. 3 and 6). The MM5 run produces a secondary PV maximum to the west of the cold frontal band. This feature may correspond to the lobe of larger PV in southwestern Oklahoma evident in Fig. 3. It is probable that the higher resolution of the MM5 run allowed these features to be distinguished.

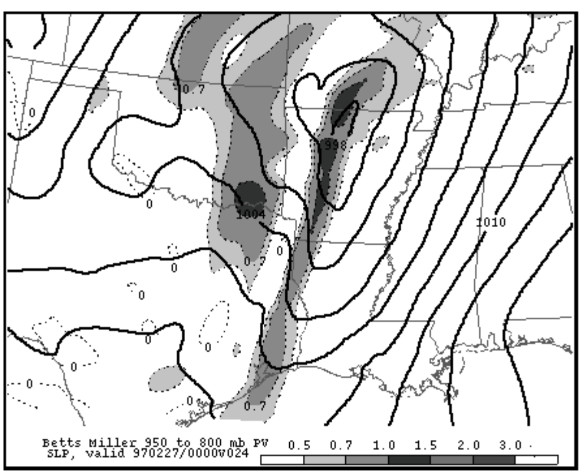

Figure 6: As in Fig. 3, except for 24-hour simulation from the control (Betts-Miller) experiment.

An experiment in which latent heating was suppressed is presented in Fig. 7. This experiment confirms the importance of diabatic processes to the lower-tropospheric PV growth; the cold-frontal PV maximum is absent in this simulation. The PV maximum over southeastern Oklahoma and northeastern Texas corresponds to the western anomaly from the control simulation. As expected, the strength of the cyclone center and the strength of the southerly flow implied by the isobars in the warm sector are reduced in comparison to the control run.

Examination of model sub-grid scale precipitation rates indicates that the convection in the MM5 runs was somewhat delayed relative to observations. As a result, differences in the lower-tropospheric PV fields attributable to CPS differences are more pronounced after 00/27. Comparison between the control simulation (Fig. 8) and an experiment in which the Kain-Fritsch CPS was utilized (Fig. 9) are therefore shown for 06/27, 30-hours into the simulation.

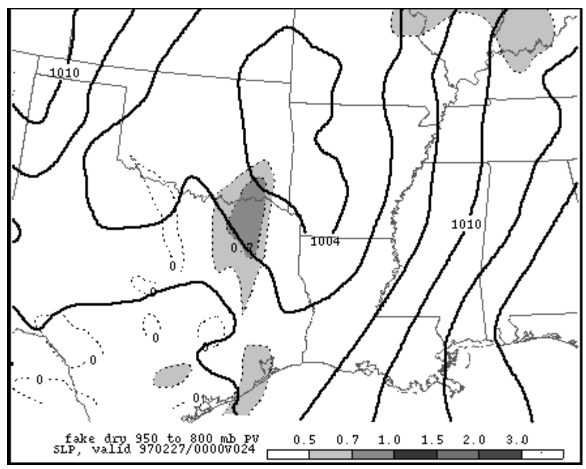

Figure 7. As in Fig. 6, except for MM5 experiment in which latent heating was suppressed.

The Betts-Miller control run indicates that the cold-frontal PV maximum has intensified by 06/27 relative to 00/27, with some PV values near the cyclone center in excess of 2 PVU at the latter time (Figs. 6 and 8). The PV band extends from Indiana southward into southern Louisiana at this time. An experiment using the Kain-Fritsch CPS produced a cold-frontal PV anomaly that was similar in structure to that in the control run, however, closer examination reveals that the band was substantially stronger in the Kain-Fritsch simulation, especially along the southern portion of the band over Louisiana (Figs. 8 and 9). Examination of total and convective precipitation also indicates that the Kain-Fritsch run produced heavier precipitation, consistent with a stronger lower PV maximum (not shown).

4. CONCLUSIONS

The MM5 experiments presented here confirm the importance of diabatic processes to the development of the cold-frontal PV maximum, and demonstrate that the intensity of this feature is somewhat sensitive to choice of CPS. The Kain-Fritsch run produced a stronger cold-frontal PV feature, especially in the southern portion of the domain. Differences between the Betts-Miller and Kain-Fritsch experiments are sufficient to warrant further investigation.

Additional experiments will be required in order to address the question of CPS variability in a more rigorous fashion. For example, explicit experiments at very high (e.g., on the order of 1 km) resolution, will be compared with the runs shown here. Additional case studies will also be required to establish the representativeness of the case studied here.

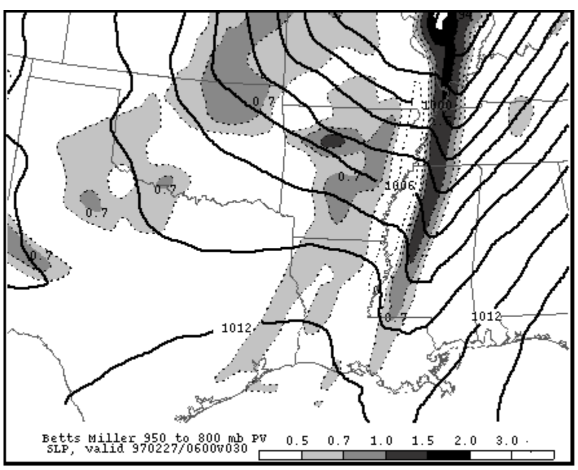

Figure 8. As in Fig. 6, except for 30-hour simulation valid 06/27.

5. ACKNOWLEDGEMENTS

This research was supported by NSF grant ATM-0079425. We thank Jim Steenburgh and Daryl Onton of the University of Utah for making the “gridder“ software available to us. The use of the MM5 model was made possible by the MMM division of NCAR, which is supported by NSF. The Unidata program is acknowledged for providing university access to gridded operational model datasets.

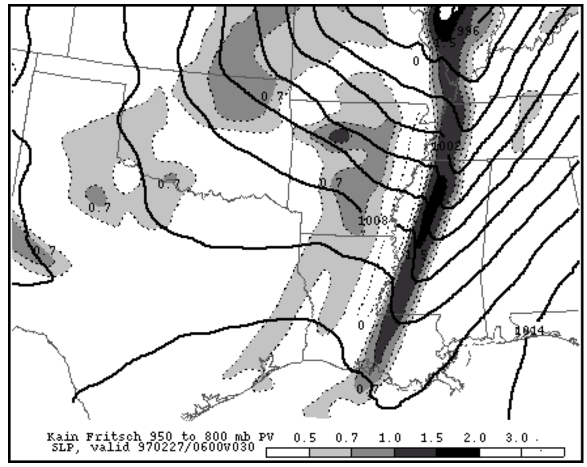

Figure 9. As in Fig. 8, except for Kain-Fritsch experiment.

6. REFERENCES

Davis, C. A., 1992: A potential-vorticity diagnosis of the importance of initial structure and condensational heating in observed extratropical cyclogenesis. *Mon. Wea. Rev.*, **120**, 2409–2428.

Davis, C. A., M. T. Stoelinga, and Y.-H. Kuo, 1993: The integrated effect of condensation in numerical simulations of extratropical cyclogenesis. *Mon. Wea. Rev.*, **121**, 2309–2330.

Lackmann, G. M., and J. R. Gyakum 1999: Heavy cold-season precipitation in the Northwestern United States: Synoptic climatology and an analysis of the flood of 17–18 January 1986. *Wea. Forecasting,* **14**, 687–700.

Raymond, D. J., 1992: Nonlinear balance and potential-vorticity thinking at large Rossby number. *Quart. J. Roy. Meteor. Soc.,* **118**, 987–1015.

Reed, R. J., M. T. Stoelinga, and Y.-H. Kuo, 1992: A model-aided study of the origin and evolution of the anomalously high potential vorticity in the inner region of a rapidly deepening marine cyclone. *Mon. Wea. Rev.,* **120,** 893–913.

Stoelinga, M. T., 1996: A potential vorticity-based study of the role of diabatic heating and friction in a numerically simulated baroclinic cyclone. *Mon. Wea. Rev.,* **124,** 849–874.

Wang, W. and N. L. Seaman 1997: A comparison study of convective parameterization schemes in a mesoscale model. *Mon. Wea. Rev.,* **125,** 252–278.